

# SAR SPECKLE SIMULATION

Regine Bolter, Margrit Gelautz, Franz Leberl  
Institute for Computer Graphics  
Technical University Graz  
Münzgrabenstraße 11  
A-8010 Graz, Austria  
e-mail: bolter@icg.tu-graz.ac.at  
Commision II, Working Group 4

**KEY WORDS:** Remote Sensing, Simulation, SAR, Speckle

## ABSTRACT

After a short introduction to the principles of SAR speckle generation and its statistical properties, we give a review of different speckle simulation methods described in literature. Then, the implementation of some selected algorithms is described, and their performance is tested on simulated ERS-1 images. Special attention is paid to the modeling of multiple looks, and the differences between image pixel size and original radar ground resolution. A chi-square distribution and a Rayleigh distribution with multiple file averaging were found to produce the most realistic results.

## KURZFASSUNG

Nach einer kurzen Einführung über die Prinzipien der SAR-Speckle Entstehung und einer Beschreibung der statistischen Eigenschaften geben wir einen Überblick über verschiedene Speckle-Simulationsmethoden, die in der Literatur beschrieben sind. Dann wird die Implementierung einiger ausgewählter Algorithmen beschrieben, und ihre Performance wird anhand von simulierten ERS-1 Bildern geprüft. Dabei wird besonderes Augenmerk auf die Modellierung von Multiple Looks, sowie der Unterschiede zwischen Bildpixelgröße und ursprünglicher Bodenaufklärung des Radars, gelegt. Die Verwendung einer chi-square Wahrscheinlichkeitsverteilung, sowie einer Rayleigh-Verteilung mit Mittelung über Mehrfachfiles, lieferten die Ergebnisse mit der größten Realitätstreue.

## 1 INTRODUCTION

SAR (Synthetic Aperture Radar) simulation is an important tool for the development and testing of SAR image processing algorithms, since simulation provides inexpensive and flexible test material, which often cannot be obtained from other sources. Furthermore, in those cases where no ground truth data is available, e.g. planetary mapping, simulation is often the only means of verification. In order to make the simulated imagery look as realistic as possible, the proper treatment of SAR speckle noise is an important issue. This is to avoid situations where image analysis algorithms perform well on simulated data, however fail in their actual application to real SAR data.

Speckle is a physical effect, which occurs when coherent light is reflected from an optically rough surface. In remote sensing SAR sensors, speckle results from the need to create the radar image with coherent radiation. A single resolution cell typically covers a 25m x 25m area on the ground. The transmitted wave length onto that resolution cell is only a few centimeters. Due to the texture and roughness within a resolution cell numerous targets exist that produce the radar echo. The characteristic speckle effect of radar images results from the destructive and constructive interferences among the echoes of individual surface scatterers within a resolution cell. Therefore the resultant pixel can differ extremely from its average gray value. These gray value variations between adjacent pixels lead to the typical grainy appearance of SAR images.

The nature of speckle can be interpreted as a random effect. This in turn can be reduced by averaging adjacent pixels. If the resolution in range direction is lower than in azimuth direction, a multiple look image can be created by averaging several image range lines so that the resulting pixels cover a

square area on the ground. Creating a multiple look image reduces the speckle effect, but at a cost of reduced azimuth resolution.

The interpretation of speckle as a random effect leads to statistical descriptions as given by, e.g., [Goodman, 1975]. The magnitude of the resultant speckle field follows a Rayleigh probability distribution, the phases are uniformly distributed, and the speckle intensities can be described by a negative exponential distribution. The analysis also shows that  $N$  non-coherent "look-averaging" results in a density function for intensity that is chi-squared with  $2N$  degrees of freedom. As  $N$  increases, this distribution approaches a normal distribution.

When dealing with SAR simulation, we have to distinguish between *raw signal simulators* and *SAR image simulators*. In raw signal simulators, first the signal received by the sensor is generated, and then this signal is passed through an appropriate Doppler processor to produce the final SAR image. Speckle is considered at signal level, by simulating the physical process of adding up the different scatterers falling into one resolution cell. A prerequisite for this technique is a high resolution Digital Elevation Model (DEM) which contains information about the surface micro structure. In SAR image simulators, information about the DEM and the imaging geometry is used to compute the gray values of the SAR image directly, without intermediate signal representation. Speckle is added to the final image by appropriate modeling of its statistical properties. The absence of speckle in radar shadows needs also be taken into account.

In the next section, several SAR speckle simulation techniques presented in the literature are reviewed. Afterwards, we describe and discuss the implementation of some selected algorithms, which were embedded into an already existing SAR

image simulator. The results obtained from application to ERS-1 images are presented and evaluated by visual comparison with the corresponding real image.

## 2 SPECKLE SIMULATION METHODS

Whereas a considerable body of literature deals with SAR speckle filtering, the topic of SAR speckle simulation can only be found in a limited number of publications.

An early work suited to the analog representation of radar images on film was published by [Holtzman, 1978]. In 1978, when this paper was published, the intensity of the video signal exiting the receiver was recorded on film, and this process is modeled by the simulator. The starting point for the radar simulation imaging model (gray tone equation) is the prediction of the power reflected from each resolvable ground element (resolution cell). It is assumed that the ground can be modeled as a collection of homogeneous regions, each at least the size of a resolution cell.

After the ground truth data base (terrain feature model) of the described site has been specified, the reflectivity data for the various categories included in the data base have been obtained, and the complex geometry relating the radar platform to the scene has been determined, the imaging model is used to calculate the power reflected from the ground back to the radar for each pixel in the image. The return power from a single resolution cell is given by the radar equation

$$\overline{P_R} = \frac{P_t G^2 \lambda^2 \sigma^0 A}{(4\pi)^3 R^4} \quad (1)$$

where the average transmitted power is represented by  $P_t$ , the two way gain of the transmitting/receiving antenna is given by  $G^2$ , and the transmitted wavelength is given by  $\lambda$ ; the reflectivity model, which is a function of wavelength and local incidence angle, among others, is  $\sigma^0$ ; the area of the resolution cell on the ground being sensed is  $A$ ; and the distance from the antenna to the resolution cell being sensed is  $R$ . Speckle statistics, depending on the number of independent looks, are considered at this level:

$$P_R = \left( \frac{\overline{P_R}}{2N} \right) (Y) \quad (2)$$

where  $P_R$  is the expected value of the return power from a resolution cell,  $Y$  is a random number with a standard chi-square distribution having  $2N$  degrees of freedom, and  $N$  is the number of independent looks. When the number of independent samples being averaged is large, (2) becomes

$$P_R = \overline{P_R} \left( 1 + \frac{z}{\sqrt{N}} \right) \quad (3)$$

where  $z$  is a Gaussian random variable with zero mean and unit variance. This return power calculated for each resolution cell is coded into one pixel in the simulated image using the gray tone equation:

$$G_R = G_{RC} + \frac{2^{n-1}}{x} (\gamma \lg P_R + \gamma \lg M + \lg K - \lg[(I_C)^\gamma K_C]) \quad (4)$$

where  $2^{n-1}$  denotes the number of possible gray values,  $x$  is the base 10 logarithm of the dynamic range of the radar signal being mapped into the linear range portion of the film

dynamic range, and  $M$  is the transfer function of the radar receiver;  $K$  is a constant depending upon the exposure time and the film processing and development, and  $\gamma$  is a positive constant representing the slope of the linear portion of the film curve of density versus logarithm of exposure;  $I_C$ ,  $K_C$ ,  $G_{RC}$  are calibration parameters.

The graytone equation (4) represents the conversion of the signal returned from each resolution element into the appropriate gray value for each image pixel after the elevation profile, dielectric categories, and spatial relationships of the various cells have been properly considered. Multiple looks are also taken into account.

The approach to simulation of SAR image products described by [Rainey, 1988] departs from most other simulation algorithms in the method of speckle generation. Speckle is prepared corresponding to the frequency, weightings and look averaging strategy of the radar-processor combination desired, and then multiplied by the source scene data preconditioned by the desired resolution. The method allows output pixel spacings to be specified independent of more fundamental system parameters. This accounts for the fact that, when dealing with SAR, pixel and resolution are two quite different concepts and quantities. Fundamental SAR spatial behavior occurs at the resolution cell level, whereas digital image representation is at pixel level. So, the authors argue that it is not sufficient to simulate speckle simply by imposing a random distribution on each pixel, and treating adjacent pixels as statistically independent. Their approach is as follows:

### 1. Image File

- (a) From a source file of ideal imagery, the reflectivity map, create one unspeckled image by convolving the source against the (desired) two-dimensional impulse response function.
- (b) If additive noise is to be included, add a constant to the resulting intermediate image.

### 2. Speckle File

- (a) Prepare  $N$  files each of which is a complex Gaussian pseudo-random field, essentially a 'white noise' source. Adjacent samples should be statistically independent.
- (b) Bandpass filter each file with the two-dimensional frequency spectra corresponding to the radar and processor to be simulated. Each filter should be weighted and overlapped as per the described system.
- (c) Square law detect the filter outputs, and sum, again using any weighting representative of the system. Normalize.
- (d) Store the resulting real variates as a 'speckle file'. This file, of course, is also in two dimensions.

### 3. Simulation

- (a) Subsample the image file and the speckle file to match the desired pixel spacing.
- (b) Pixel by pixel, multiply the two files together to create the final speckled image files.

For a given radar-processor combination the computationally expensive creation of the speckle file is computed only once.

To simulate an image of a new area, only the image file steps (a) and (b) and the simulation steps (a) and (b) have to be recomputed, provided the radar-processor combination remains. The texture of simulated image speckle is related to the resolution of the radar. It is represented mathematically by the autocorrelation function of the speckle. The intensity distribution of the speckle is related to the number and independence of the looks. The authors proved with a number of test speckle data sets that the parameters of the speckle (autocorrelation shape and intensity distribution) vary with, and only with the appropriate parameters.

This approach, which requires exact sensor specifications, is very accurate in considering the spatial characteristics of speckle noise. Multiple looks as well as the difference between pixel size and resolution cell are taken into account.

More recently, the implementation of speckle in a raw signal simulator is described by [Franceschetti, 1992]. In the Synthetic Aperture Radar Advanced Simulator (SARAS) presented, the statistical features are implemented on the physical model and not on the final image. The height profile of the scene is approximated by square plane facets, large in terms of the incident wavelength, but small when compared to the resolution cell. Each facet is characterized by the coordinates of its vertices and by the electro-magnetic parameters (permittivity and conductivity) of the underlying material. The computation of individual facet backscattering takes into account local incidence angle, polarization of the incident wave, the facet's roughness and any shadowing effect, if present. The small scale statistics are considered by a large number of uncorrelated scatterers per facet, so that the facets' return is characterized by a uniform phase and Rayleigh amplitude distribution. The correct large scale statistical simulation due to irregularities of the macroscopic terrain profile is modeled by associating with each facet a random displacement of three of its four vertices. The small and large scale characterization of the electro-magnetic scattering results in the inclusion of the appropriate statistics of the speckle on the raw signal and, after computation, on the image. The simulator output, which is the SAR raw signal, is the appropriate superposition of returns from each facet. The efficient summation of all returns is accomplished via two-dimensional FFT code and an asymptotic evaluation of the system transfer function.

This simulator is based on a physical model which takes into account the elevation profile together with shadows and lay-over, terrain electromagnetic properties together with frequency and polarization dependence, and small as well as large scale statistics. With exact specifications, various different sensor types can be handled by this simulator.

[Wiles, 1993] deals with a particular data set, namely Magellan images of planet Venus. Simulated imagery is used to test a correlation algorithm developed for the automated detection of volcanos on Venus. A control experiment is carried out to calibrate the ability both of humans and the machine to identify small 'pit like' features in the presence of speckle noise. To achieve this, it was necessary to produce simulated radar images of synthetic terrain, designed to resemble Magellan imagery as closely as possible. This procedure involved several stages:

1. Production of artificial terrain: A Digital Elevation Model (DEM) was produced which would closely resemble the morphology of volcanic pits on Venus.

2. Radar image simulation: A radar image simulation described in [Leberl, 1990] was employed, the effect of speckle was modeled separately and added to the final image (see below).
3. Scene generation: Artificial scenes were generated for a whole range of pit diameters from 2 - 16 pixels. The pits were at a random location within the scene.
4. Addition of speckle: The effects of speckle were simulated by using a Rayleigh random number generator to produce a speckle image of the same size as the simulated image, with a mean value of 1.0. To incorporate multiple looks, several such images were generated using different random number seeds. For simulated Magellan images, five of the speckle images were averaged together. Finally, since speckle noise is multiplicative, the artificial scene was multiplied by the five-average speckle image pixel by pixel.
5. Resolution degradation: The last stage of the data simulation was to emulate the resampling of Magellan images. Therefore a 3x3 local neighborhood blurring was employed. The blurring kernel was chosen so as to mimic the resampling of typical Magellan resolution cells of 150m x 110m into 75m x 75m pixels.

With the so generated synthetic data, [Wiles, 1993] showed that their correlation algorithm performed at least as good as human observers. The speckle simulation model used takes both multiple looks and the difference between pixel size and resolution cell into consideration.

### 3 IMPLEMENTATION AND RESULTS

Starting point of our implementation was an already existing SAR image simulator which uses a DEM and knowledge about the sensor flight path to generate a simulated noise-free image. Therefore, we only deal with the generation of SAR speckle at the image level, by modeling its statistical properties, as opposed to the more basic incorporation of speckle at the signal level. Due to the multiplicative nature of speckle, the simulated noise-free image is then multiplied by a separately generated speckle file. The simulation program used to produce the noise-free image is part of the RSG software package of JOANNEUM RESEARCH [JR, 1993]. The algorithms were implemented in [IDL, 1994] (Interactive Data Language). Performance evaluation was carried out by visual comparison with real SAR images.

Figure 1 shows a section of a real ERS-1 image of the Ötztal test site, a highly mountainous terrain in Tyrol, Austria. This image was processed using 3 independent looks. The size of a resolution cell on the ground is 25m x 25m, and the final pixel size is 12.5m x 12.5m. A simulated image of the same scene, but without speckle noise, can be seen from Figure 2. The goal is now to reduce the differences between the two images by including simulated speckle noise.

Since the statistical properties of speckle noise can be described by a Rayleigh probability distribution, our first approach was to multiply the simulated image pixel by pixel with a speckle file of the same size with Rayleigh distributed random numbers. A Rayleigh distributed random numbers  $Z$  can be generated from a uniformly distributed random number  $u$ , as provided in IDL, by using

$$Z = \sqrt{-2\sigma^2 \ln(1-u)} \quad (5)$$

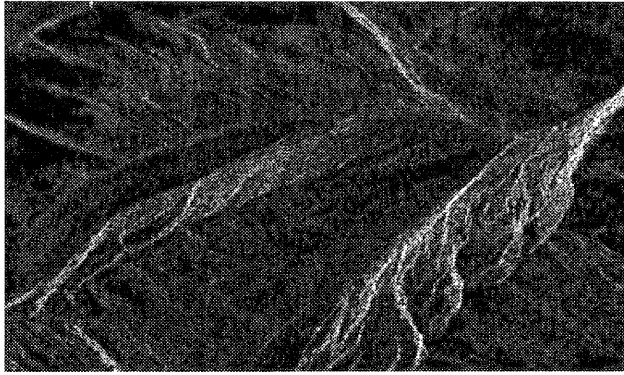


Figure 1: A detail of an ERS-1 scene of the Ötztal test site. The area covers approximately 9km x 5km. The scene was illuminated from the left, at a look angle of 23 deg. Copyright esa.

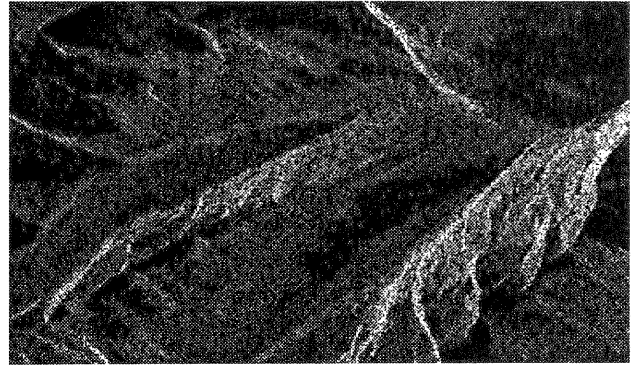


Figure 3: A simulated ERS-1 image of the scene shown in Figure 1. Speckle was simulated by generating one speckle file with Rayleigh random numbers of the same size as the simulated image and multiplying them pixel by pixel.

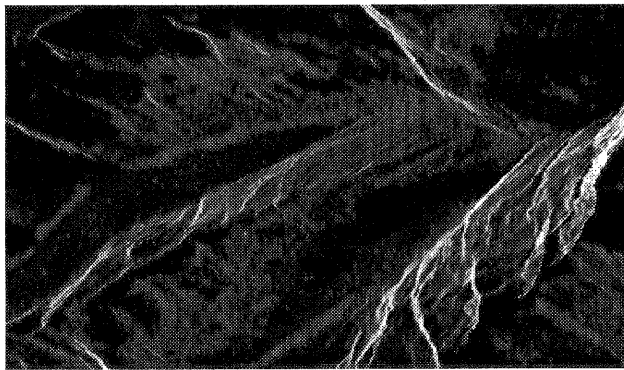


Figure 2: A noise-free simulated ERS-1 image of the scene shown in Figure 1.

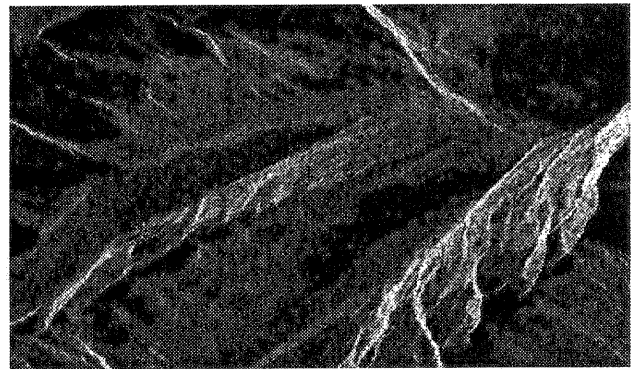


Figure 4: A simulated ERS-1 image of the scene shown in Figure 1. Multiple looks were incorporated by averaging three independently generated speckle files with Rayleigh random numbers.

where  $\sigma$  denotes a scaling factor. The very grainy appearance of Figure 3, the simulated image obtained by this algorithm, in comparison to Figure 1 arises because multiple looks were not taken into consideration.

So our next step was to incorporate multi-looking. In the simulator of [Wiles, 1993], multiple looking was considered by generating several speckle files with a Rayleigh random number generator, where the number of generated speckle files depends on the number of independent looks. These speckle files are then averaged together, and finally multiplied pixel by pixel with the simulated noise-free image. Figure 4 shows the resultant image for three independent looks, the same number that was used for the original ERS-1 image.

Another possibility, as described by e.g. [Holtzman, 1978], is to multiply the simulated image with a chi-square distributed speckle file with  $2N$  degrees of freedom, where  $N$  denotes the number of independent looks. The chi-square distribution is a special gamma distribution with parameters  $\gamma(\frac{n}{2}, \frac{1}{2})$ . The gamma distribution random number generator was implemented as described in [Press, 1986].

The visual impression of the image obtained by using the chi-square distributed speckle file (Figure 5) and the image generated by averaging three Rayleigh distributed speckle files (Figure 4) was judged by several test persons. It was found that the differences between the two images were minor, with the approach based on chi-square distribution delivering slightly

better results. Both images were judged to be clearly superior to the image from Figure 3, which was generated without accounting for multiple looks.

What we have not considered until now is the difference between resolution cell and pixel size, which results in adjacent pixels that are not statistically independent. [Wiles, 1993] deals with this problem by employing a 3x3 local neighborhood blurring. According to this, we tried several blurring kernels and finally chose:

$$\frac{1}{8} \begin{pmatrix} 0 & 1 & 0 \\ 1 & 4 & 1 \\ 0 & 1 & 0 \end{pmatrix}$$

Figure 6 shows the result of this local neighborhood blurring applied to Figure 5. Compared to the original ERS-1 image (Figure 1), the blurring seems to be not necessary in this case, the image without blurring (Figure 5) meets the original image better.

Another approach to take the resampling into account was proposed by [Rainey, 1988], as described in the previous section. The generated speckle file is not of the same size as the image, they are subsampled together to match the desired pixel spacing. We implemented this idea as follows. The resampling factor  $k$  is the ratio of the length of the area on the ground represented by one pixel to the length of the res-

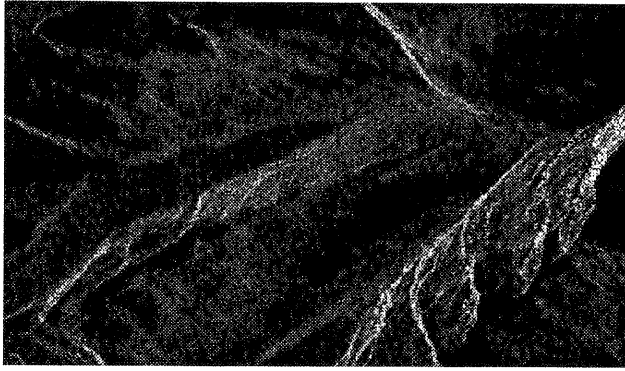


Figure 5: A simulated ERS-1 image of the scene shown in Figure 1. A chi-square distributed random number speckle file was multiplied pixel by pixel with the image from Figure 2. The number of independent looks is three.

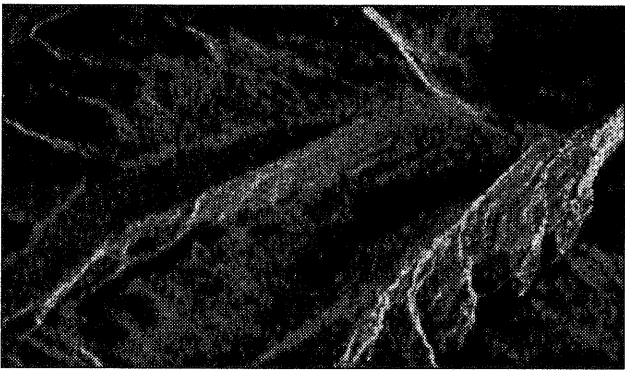


Figure 6: This image was obtained from Figure 5 using a (3x3) local neighborhood blurring.

olution cell. A speckle file was generated as described before by averaging Rayleigh distributed random numbers together, but the size of that speckle file was just  $k$  times the size of the simulated image. The speckle file was then resampled to the size of the simulated image, using a bilinear interpolation transformation, and then the simulated image and the resampled speckle file were multiplied together pixel by pixel. Figure 7 was obtained by using three independent looks and a resampling factor of  $k = 0.5$ , which is the ratio for the real ERS-1 image.

Compared to the real ERS-1 image (Figure 1), both the blurring and the resampling algorithm were found to produce results which deviate from the corresponding real image more than the images obtained without considering the difference between resolution cell and pixel size. This means that in the case of our ERS-1 simulation blurring or resampling seems not to be appropriate, because it degrades the resolution.

#### 4 SUMMARY AND CONCLUSIONS

The principles of SAR speckle generation and its statistical properties were briefly discussed in the introduction. Then, we presented four different speckle simulation methods described in the literature. Some ideas from these approaches led to our own implementation of speckle simulation into an existing SAR image simulator. In a practical application to multi-look ERS-1 images, the most realistic results were obtained by using a chi-square distribution on the one hand,

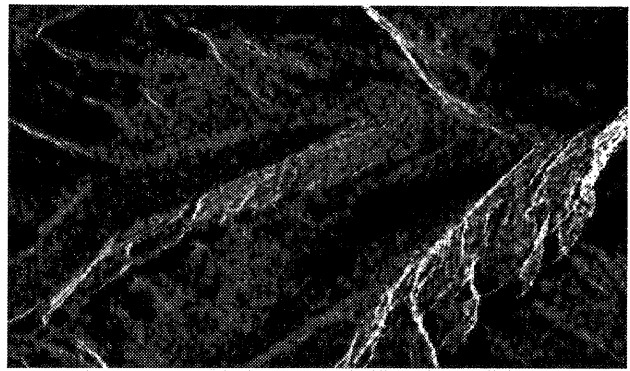


Figure 7: This image was obtained from Figure 2 by averaging three Rayleigh distributed speckle files, and applying a bilinear interpolation algorithm with a resampling coefficient of 0.5.

and a Rayleigh distribution with multiple file averaging on the other hand. The application of additional blurring or resampling algorithms, in order to account for the differences between pixel resolution and radar resolution, was found to lead to an undesired degradation in resolution.

#### ACKNOWLEDGMENTS

The authors would like to thank Dr. Helmut Rott from the Institute for Meteorology and Geophysics at the University of Innsbruck for providing the esa-ERS-1 data. Dr. Rott is Principal Investigator of the AO/Experiment A1. We gratefully acknowledge his cooperation.

This study was partly funded by the Austrian Academy of Sciences.

#### REFERENCES

- [Franceschetti, 1992] Franceschetti, G., Migliaccio, M., Riccio, D., Schirizzi, G., 1992. SARAS: A Synthetic Aperture Radar (SAR) Raw Signal Simulator. IEEE Transactions on Geoscience and Remote Sensing, Vol. 30, No. 1, pp. 110-123
- [Goodman, 1975] Goodman, J.W., 1975. Statistical Properties of Laser Speckle Patterns. In Laser Speckle and Related Phenomena, J.C. Dainty, ed. Springer Verlag, Berlin.
- [Holtzman, 1978] Holtzman, J.C., Frost, V.S., Abbot, J.L., Kaupp, V.H., 1978. Radar Image Simulation. IEEE Transactions on Geoscience and Remote Sensing, Vol. GE-16, No. 4, pp. 296-303
- [IDL, 1994] IDL (Interactive Data Language) User Manual, Version 3.6.1a, 1994. Research Systems Inc., Boulder, CO.
- [JR, 1993] JOANNEUM RESEARCH, 1993. RSG - Remote Sensing Software Package Graz, Software User Manual, Release No. 3.0, Institute for Digital Image Processing.
- [Leberl, 1990] Leberl, F.W., 1990. Radargrammetric Image Processing. Artech House, Norwood, MA.
- [Press, 1986] Press, W.P., Flannery, B.P., Teukolsky, S.A., Vetterling, W.T., 1986. Numerical Recipes. Cambridge University Press, Cambridge, pp. 191-209
- [Rainey, 1988] Rainey, R.K., Wessels, G.J., 1988. Spatial Considerations in SAR Speckle Simulation. IEEE Transactions on Geoscience and Remote Sensing, Vol. 26, No. 5, pp. 666-671

[Wiles, 1993] Wiles, C.R., Forshaw, M.R.B., 1993. Recognition of Volcanos on Venus using Correlation Methods. Image and Vision Computing, Vol. 11, No. 4, pp. 188-196